Electronic Supplementary Material (ESI) for New Journal of Chemistry.

SUPPORTING INFORMATION

Electronic state regulation induced by the strong metal-support interactions boosts the performance of alcohol oxidation reactions

Yaheng Wang, Fengshou Yu, Peng Guo, Yang You, Zhihao Feng, Yuzhuo Zhou, Bo Zhang, Shaobo Zhang and Lu-Hua Zhang**

National-Local Joint Engineering Laboratory for Energy Conservation in Chemical Process Integration and Resources Utilization, School of Chemical Engineering and Technology, Hebei University of Technology, Tianjin 300130, P. R. China

E-mail: luhuazhang@hebut.edu.cn (L.-H. Zhang); yfsh@hebut.edu.cn (F. Yu)

Materials.

3-Aminophenol (3-AP, 98%) and hexamethylenetetramine (HMT,99.5%) were purchased from Sinopharm Chemical Reagent Co. Potassium palladium (II) chloride (K_2PdCl_4, Pd≥32.6%), and silver nitrate ($AgNO_3$,99.8%) were got from Aladdin. Sodium borohydride ($NaBH_4$,98%), dicyandiamide (DCDA,99.8%), Pluronic F127 (98%), carbon black (Vulcan XC-72) and Sodium hydroxide (NaOH,96%) were brought from Tianjin Fuchen (Tianjin, China). All chemicals were used directly without any purification.

Synthesis of PdAg@N_xC Sample.

In a typical preparation of the PdAg@$N_{15.6}$C, 360 mg of 3-AP, 90 mg DCDA and 15.6 mg of K_2PdCl_4 were added to 50 mL of DI water and sonicated for 10 min, recorded as solution A. 160 mg of F127 and 280 mg of HMT were dispersed in 30 mL of DI water and allowed to stand for 20 min, recorded as solution B. Subsequently, A is mixed with B and stirred slowly for 25 min at 30 °C. The mixed solution was then transferred to a 200 mL Teflon container which was sealed and kept at 80 °C for 24 h. Wash the precursor by filtration after cooling the solution to room temperature. Dissolving a quarter of the precursor in 50 mL of DI water, adding 3 mL of ammonia to adjust the PH, add 2.03 mg of $AgNO_3$ and stir for 2 h. The samples were washed by filtration again to pH=7, and finally freeze-dried at -40 ℃, 15 Pa. The dried precursor was pyrolyzed for 3 h at 400 ℃ with the 10% H_2 + 90% Ar atmosphere, then heated to 600 ℃ and kept 1 h. Finally, the products were treated for 4 h at 240 ℃ in tube furnace under the O_3/air flow. The resulting catalyst was named as PdAg@$N_{15.3}$C. As listed in **Table S1**, PdAg@$N_{14.3}$C and PdAg@$N_{13.6}$C were synthesized by adding different amounts of DCDA as additional N source.

Synthesis of PdAg@C Sample.

Typically, 13.3 mg $PdCl_2$ and 12.7 mg $AgNO_3$ were mixed well, and a total of 50 mg carbon black was then added while grinding for 30 min. Next, 12 mg NaOH was added and the mixture was grinded for 30 min, followed by adding 22.7 mg $NaBH_4$ and another 30 min grinding. After several washing with acetone-deionized water (1:1) and drying at 60 ℃ under vacuum, PdAg@C was obtained.

Physicochemical Characterization.

scanning electron microscopy (SEM) image was captured on a Tescan MIRA LMS and transmission electron microscopy (TEM) images were acquired on a FEI Talos F200XG2 AEMC. Before characterization, 3 mg of catalyst was dispersed in 30 mL of ethanol absolute, and sonicated for 30 min and then dropped onto a microetching copper mesh. ICP-MS was derived by America Aglient 7800 (MS). X-Ray Diffraction (XRD)

patterns were taken on Rigaku Ultima IV microscope, and the catalyst powder was sprinkled on a microscope carrier film and a sufficient amount of ethanol absolute was added to make a thin slurry of the powder, which was spread evenly and tested after the ethanol absolute had evaporated. X-ray photoelectron spectroscopic (XPS) spectra of the samples were measured on an America Thermo Scientific ESCALAB 250Xi and Data analyzed by XPS41 software and data was calibrated according to C1 s. UV photoelectron spectroscopy (UPS) were measured on a PHI5000 VersaProbe III SCA instrument.

Electrochemical measurements.

All electrochemical experiments were operated in a standard three-electrode steup (CHI 660E, Shanghai Chenhua, China). A glassy carbon electrode, platinum electrode and a saturated Hg/HgO electrode were used as the working, counter electrode and reference electrode, respectively. For the preparation of the working electrode, the details are as follows: 4 mg of the catalyst was dissolved in 760 μL of alcohol/water solution (volume ratio: 1/1), then 40 μl of Nafion solution (5 wt%) was added and homogeneously dispersed by ultrasonication for 20 min, finally 20 μL of ink was taken and dropped onto the surface of the glassy carbon electrode. The electrochemically active surface area (ECSA, m^2 g^{-1}_{Pd}) of the tested electrocatalysts was calculated based on the below equation:

$$ECSA = Q/(0.405 \times W_{Pd})$$

where W_{Pd} is the quantity of Pd dispersed on the glassy carbon (mg cm^{-2}), Q represents the reduction charges of the PdO (mC) by integrating the peak area of PdO, 0.405 is the conversion factor for an oxide monolayer reduction (mC cm^{-2}).

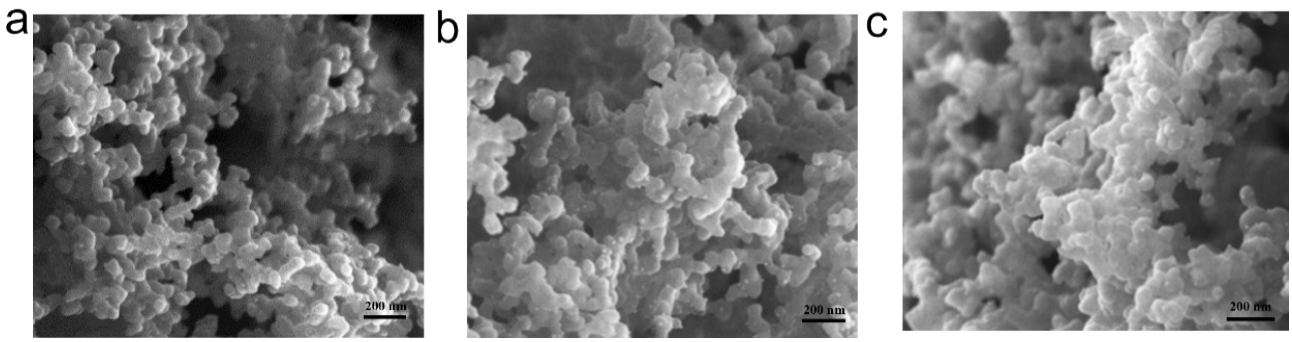

Fig. S1. (a) The SEM images of PdAg@$N_{15.3}$C; (b) The SEM images of PdAg@$N_{14.3}$C; (c) The SEM images of PdAg@$N_{13.6}$C.

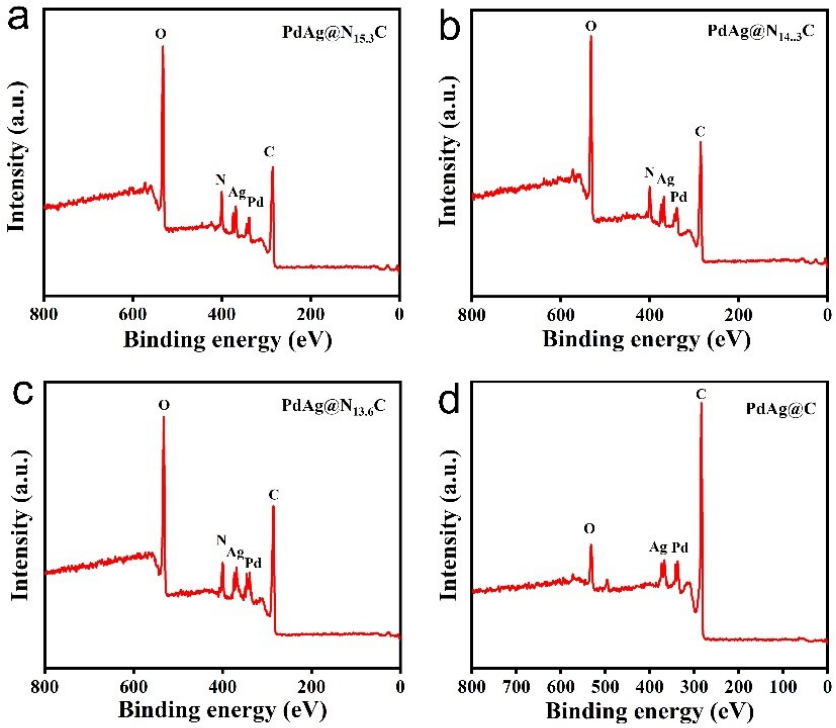

Fig. S2. XPS spectra for the survey scan of (a) PdAg@$N_{15.3}$C, (b) PdAg@$N_{14.3}$C (c) PdAg@$N_{13.6}$C and (d) PdAg@C.

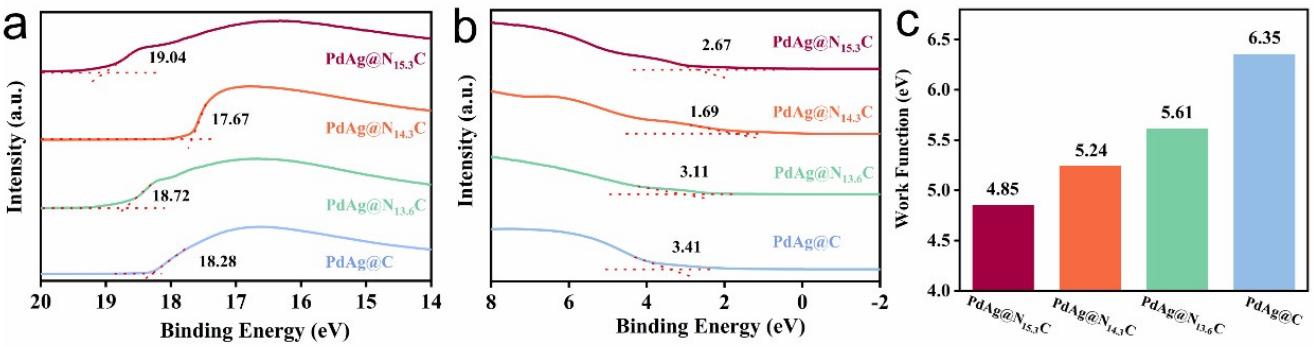

Fig. S3. UPS spectra in the secondary electron cut-off ($E_{cut\text{-}off}$) (a) and onset (E_F) energy (b) regions of PdAg@N_xC; (c) The work function of PdAg@N_xC, as calculated by the equation of Φ=21.21 eV - ($E_{cut\text{-}off}$ - E_F).

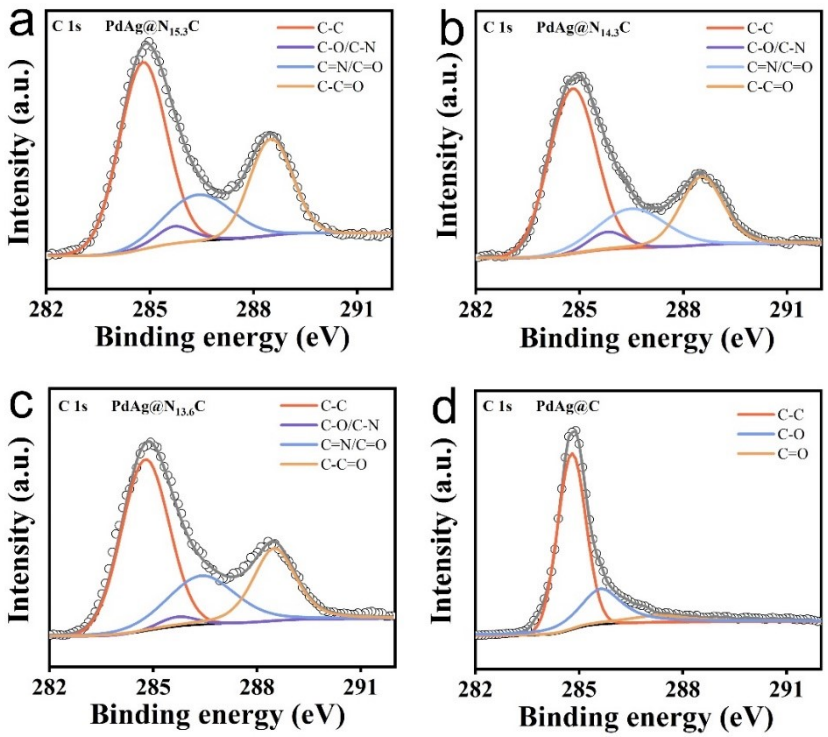

Fig. S4. XPS spectra for the survey scan of (a) PdAg@$N_{15.3}$C, (b) PdAg@$N_{14.3}$C (c) PdAg@$N_{13.6}$C and (d) PdAg@C.

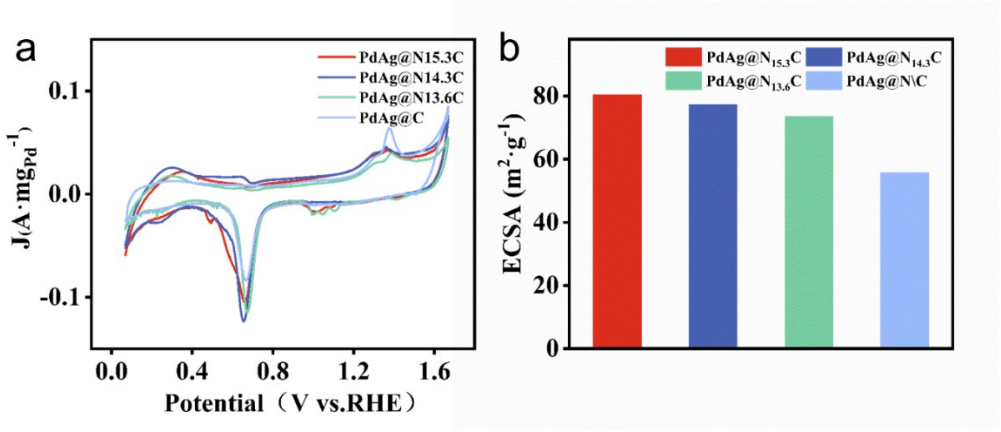

Fig. S5. (a) CV curves of PdAg@$N_{15.3}$C, PdAg@$N_{14.3}$C, PdAg@$N_{13.6}$C and PdAg@ C, recorded in Ar-saturated 1.0 M KOH. (b) ECSA of PdAg@$N_{15.3}$C, PdAg@$N_{14.3}$C, PdAg@$N_{13.6}$C and PdAg@C.

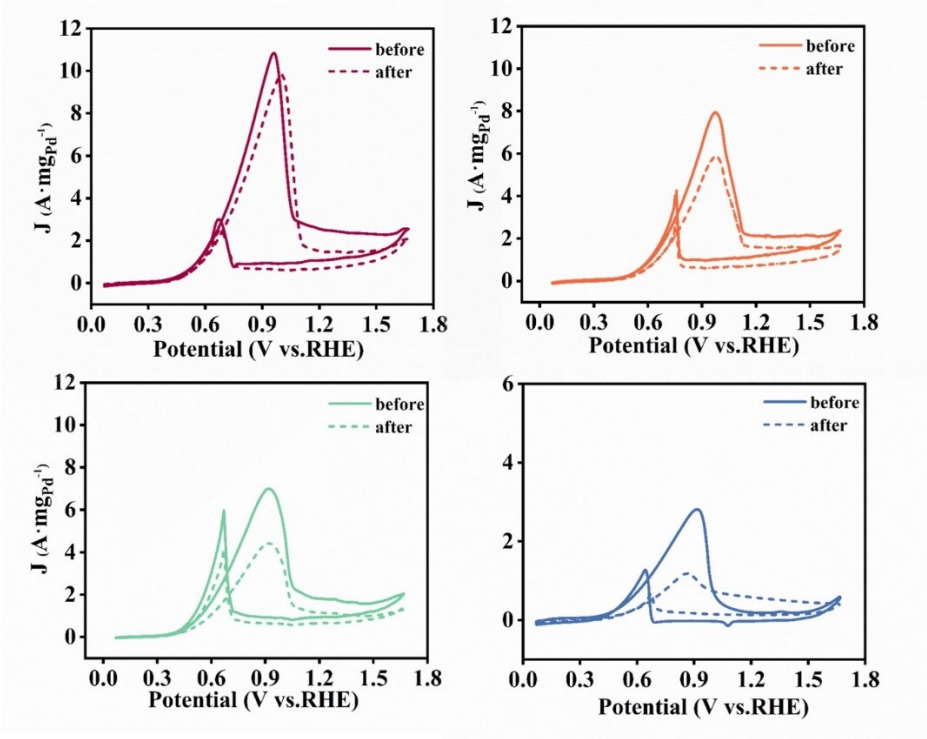

Fig. S6. CVs curves before and after 700 cycles of stability tests for (a) PdAg@$N_{15.3}$C, (b) PdAg@$N_{14.3}$C (c) PdAg@$N_{13.6}$C and (d) PdAg@C catalysts in 1.0 M KOH + 1.0 M EtOH aqueous solution at a scan rate of 50 mV s^{-1}.

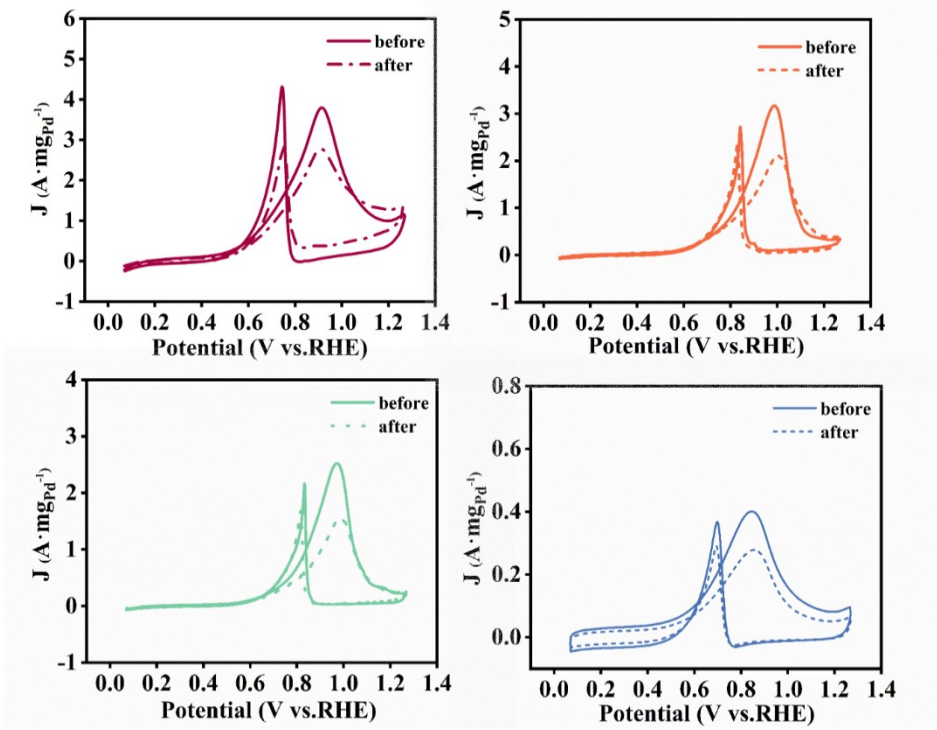

Fig. S7. CVs curves before and after 700 cycles of stability tests for (a) PdAg@$N_{15.3}$C, (b) PdAg@$N_{14.3}$C (c) PdAg@$N_{13.6}$C and (d) PdAg@C catalysts in 1.0 M KOH + 1.0 M MeOH aqueous solution at a scan rate of 50 mV s^{-1}.

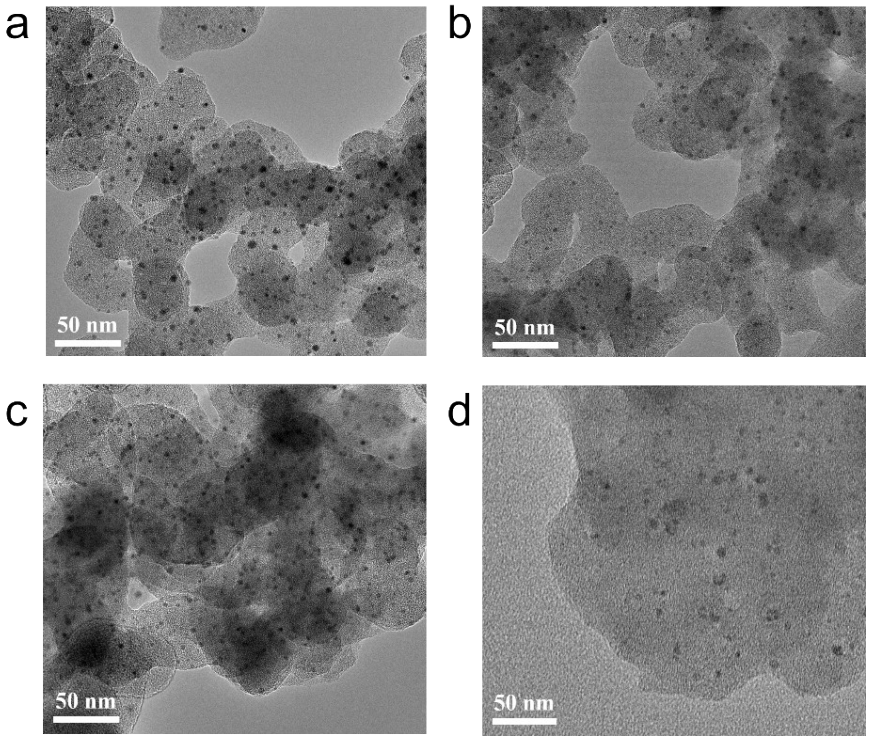

Fig. S8. (a) The TEM images of PdAg@$N_{15.3}$C after AOR; (b) The TEM images of PdAg@$N_{14.3}$C after AOR; (c) The TEM images of PdAg@$N_{13.6}$C after AOR; (d) The TEM images of PdAg@ C after AOR.

Table S1. The contents of DCDA for the preparation of precursors.

Sample	DCDA (mg)
PdAg@$N_{15.3}C$	90
PdAg@$N_{14.3}C$	60
PdAg@ $N_{13.6}C$	30

Table S2. Element contents of PdAg@NxC, PdAg@C samples estimated from XPS analysis.

Sample	Pd (at. %)	Ag (at. %)	N (at. %)	C (at. %)
PdAg@$N_{15.3}C$	1.19	1.14	15.28	82.39
PdAg@$N_{14.3}C$	1.23	1.22	14.3	83.25
PdAg@$N_{13.6}C$	1.12	1.11	13.64	84.13
PdAg@ C	1.3	1.27	0	97.43

Table S3. The contents of Pd and Ag in PdAg@NxC, PdAg@C samples determined by ICP-MS.

Sample	Pd (wt. %)	Ag (wt. %)
PdAg@$N_{15.3}C$	2.5	1.58
PdAg@$N_{14.3}C$	2.6	1.72
PdAg@$N_{13.6}C$	3.1	1.67
PdAg@ C	4.3	3.2

Table S4. Characteristic peak fitting of Pd 3d XPS spectra.

			$PdAg@N_{15.3}C$	$PdAg@N_{14.3}C$	$PdAg@N_{13.6}C$	PdAg@C
Pd (II)	$3d_{5/2}$	PEAK	338.17	338.36	338.52	338.77
		FWHM	1.64	1.64	1.64	1.64
	$3d_{3/2}$	PEAK	343.57	343.76	344.02	344.17
		FWHM	1.34	1.34	1.34	1.34
Pd (0)	$3d_{5/2}$	PEAK	336.17	337.06	336.22	336.87
		FWHM	1.6	1.6	1.6	1.6
	$3d_{3/2}$	PEAK	341.87	342.16	342.92	342.37
		FWHM	1.6	1.6	1.6	1.6

Table S5. Characteristic of C 1s peak fitting of XPS spectra.

			$PdAg@N_{15.3}C$	$PdAg@N_{14.3}C$	$PdAg@N_{13.6}C$
N 1s	Graphitic N	PEAK	400.95	400.85	400.8
		FWHM	1.59	1.59	1.59
	Pyrrolic N	PEAK	399.65	399.6	399.5
		FWHM	1.34	1.34	1.34
	Pyridinic N	PEAK	398.25	398.2	398.1
		FWHM	1.07	1.07	1.07

Table S6. Comparison of MA and SA for EOR performance.

Catalysts	Electrolyte	MA ($A\ mg_{PGM}^{-1}$)	SA ($mA\ cm^{-2}$)	Ref.
$Pd@N_{15.3}C$	**1 M KOH+1 M CH_3CH_2OH**	**10.8**	**13.2**	**This work**
3D Au@Pt-Pd hemispherical nanostructures	1 M KOH + 1 M CH_3CH_2OH	3.18	3.66	[1]
Ni-modified Pt nanowires	1 M KOH + 1 M CH_3CH_2OH	5.60	*NA*	[2]
Porous PdPtNi nanosheets	1 M KOH + 1 M CH_3CH_2OH	5.12	4.16	[3]
PdPtCu nanosheets	1 M KOH + 1 M CH_3CH_2OH	3.79	*NA*	[4]
Star-like PdPtNi nanostructures	1 M KOH + 1 M CH_3CH_2OH	1.20	0.21	[5]
PdAu nanospheres	1 M KOH + 1 M CH_3CH_2OH	5.113	10.3	[6]
PdAgCu mesoporous nanospheres	1 M KOH + 1 M CH_3CH_2OH	4.64	*NA*	[7]

PdCu porous nanomeshes	1 M KOH + 1 M CH_3CH_2OH	3.22	*NA*	[8]
PtRhNi nanoassemblies	1 M NaOH + 1 M CH_3CH_2OH	1.39	7.97	[9]
3D PdCu nanosheets	1 M KOH + 1 M CH_3CH_2OH	4.30	6.60	[10]
PdAg nanodentrides	1 M KOH + 1 M CH_3CH_2OH	2.60	*NA*	[11]

Table S7. Comparison of MA and SA for MOR performance.

Catalyst	Electrolyte	MA (A mg_{PGM}^{-1})	SA (mA cm^{-2})	Ref.
Pd@$N_{15.3}C$	**1 M KOH+1 M CH_3OH**	**3.6**	**4.7**	**This work**
6 nm Pd Networks	1 M KOH+1 M CH_3OH	1.38	8.4	[12]
Pd/Te catalyst	1 M KOH+1 M CH_3OH	2.30	3.1	[13]
Pd_4Pb nanosheet array	1 M KOH+1 M CH_3OH	1.74	2.9	[14]
Pd NW @ CuOx	1 M KOH+1 M CH_3OH	0.54	6.3	[15]
Pd_4Sn nanowires	1 M KOH+0.5 M CH_3OH	1.04	*NA*	[16]
$Pd_{59}Cu_{33}Ru_8$ Nanosheets	1 M KOH+1 M CH_3OH	1.66	4.7	[17]
Pd-CeO_2 NMCs	1 M KOH+1 M CH_3OH	1.45	3.1	[18]
Pt_1Ni_1/ C	1 M KOH+1 M CH_3OH	1.75	4.8	[19]
PtCu nanoframes	0.5 M KOH+1 M CH_3OH	2.26	18.2	[20]
Porous Pt nanotubes	1 M KOH+1 M CH_3OH	2.33	5.1	[21]
PtAuRu/rGO	1 M KOH+1 M CH_3OH	1.60	*NA*	[22]

References

1. W. Liang, Y. Wang, L. Zhao, W. Guo, D. Li, W. Qin, H. Wu, Y. Sun and L. Jiang, 3D Anisotropic Au@Pt–Pd Hemispherical Nanostructures as Efficient Electrocatalysts for Methanol, Ethanol, and Formic Acid Oxidation Reaction, *Adv. Mater.*, 2021, **33,** 2100713.
2. M. Li, K. Duanmu, C. Wan, T. Cheng, L. Zhang, S. Dai, W. Chen, Z. Zhao, P. Li, H. Fei, Y. Zhu, R. Yu, J. Luo, K. Zang, Z. Lin, M. Ding, J. Huang, H. Sun, J. Guo, X. Pan, W. A. Goddard, P. Sautet, Y. Huang and X. Duan, Single-atom tailoring of platinum nanocatalysts for high-performance multifunctional electrocatalysis, *Nat. Catal.*, 2019, **2**, 495-503.

3. D. Wang, Y. Zhang, K. Zhang, X. Wang, C. Wang, Z. Li, F. Gao and Y. Du, Rapid synthesis of Palladium-Platinum-Nickel ultrathin porous nanosheets with high catalytic performance for alcohol electrooxidation, *J. Colloid Interface Sci.*, 2023, **650**, 350-357.
4. H. Lv, L. Sun, D. Xu, S. L. Suib and B. Liu, One-pot aqueous synthesis of ultrathin trimetallic PdPtCu nanosheets for the electrooxidation of alcohols, *Green Chemistry*, 2019, **21**, 2367-2374.
5. G. Ren, Z. Zhang, Y. Liu, Y. Liang, X. Zhang, S. Wu and J. Shen, One-pot solvothermal preparation of ternary PdPtNi nanostructures with spiny surface and enhanced electrocatalytic performance during ethanol oxidation, *J. Alloys Compd.*, 2020, **830**, 0925-8388.
6. N. Zhang, K. Zhang, J. Li, C. Ye and Y. Du, One-pot synthesis of 3D surface-wrinkled PdAu nanospheres for robust alcohols electrocatalysis, *J. Colloid Interface Sci.*, 2023, **650**, 1509-1517.
7. H. Lv, L. Sun, L. Zou, D. Xu, H. Yao and B. Liu, Size-dependent synthesis and catalytic activities of trimetallic PdAgCu mesoporous nanospheres in ethanol electrooxidation, *Chem. Sci.*, 2019, **10**, 1986-1993.
8. Y. Teng, K. Guo, D. Fan, H. Guo, M. Han, D. Xu and J. Bao, Rapid Aqueous Synthesis of Large-Size and Edge/Defect-Rich Porous Pd and Pd-Alloyed Nanomesh for Electrocatalytic Ethanol Oxidation, *Chemistry – A European Journal*, 2021, **27**, 11175-11182.
9. H. Liu, J. Li, L. Wang, Y. Tang, B. Y. Xia and Y. Chen, Trimetallic PtRhNi alloy nanoassemblies as highly active electrocatalyst for ethanol electrooxidation, *Nano Res.*, 2017, **10**, 3324-3332.
10. X. Zhao, L. Dai, Q. Qin, F. Pei, C. Hu and N. Zheng, Self-Supported 3D PdCu Alloy Nanosheets as a Bifunctional Catalyst for Electrochemical Reforming of Ethanol, *Small*, 2017, **13**, 1602970.
11. W. Huang, X. Kang, C. Xu, J. Zhou, J. Deng, Y. Li and S. Cheng, 2D PdAg Alloy Nanodendrites for Enhanced Ethanol Electroxidation, *Adv. Mater.*, 2018, **30**, 1706962.
12. Q. Zhan, R. Li, Y. Liu, K. Zhang, Y. Zheng and M. Jin, Liquid/Liquid Interface-Assisted Synthesis of Two-Dimensional Metal Networks with High-Density Planar Defects for Electrocatalysis, *Chem. Mater.*, 2022, **34**, 3960-3966.
13. W. Qiao, X. Yang, M. Li and L. Feng, Hollow Pd/Te nanorods for the effective electrooxidation of methanol, *Nanoscale*, 2021, **13**, 6884-6889.
14. H. Huang, Y. Ouyang, D. Wu, F. Wang, S. Wang, X. Meng, W. Yuan, P. Guo and L. Y. Zhang, Holey PdPb nanosheet array: An advanced catalyst for methanol electrooxidation, *Int. J. Hydrogen Energy*, 2021, **46**, 2236-2243.
15. Z. Chen, Y. Liu, C. Liu, J. Zhang, Y. Chen, W. Hu and Y. Deng, Engineering the Metal/Oxide Interface of Pd Nanowire@CuOx Electrocatalysts for Efficient Alcohol Oxidation Reaction, *Small*, 2019, **16**, 1904964.
16. Y. Zhang, B. Huang, Q. Shao, Y. Feng, L. Xiong, Y. Peng and X. Huang, Defect Engineering of Palladium–Tin Nanowires Enables Efficient Electrocatalysts for Fuel Cell Reactions, *Nano Lett.*, 2019, **19**, 6894-6903.
17. L. Jin, H. Xu, C. Chen, H. Shang, Y. Wang, C. Wang and Y. Du, Three-dimensional PdCuM (M = Ru, Rh, Ir) Trimetallic Alloy Nanosheets for Enhancing Methanol Oxidation Electrocatalysis, *ACS Appl. Mater. Interfaces*, 2019, **11**, 42123-42130.
18. Q. Tan, C. Shu, J. Abbott, Q. Zhao, L. Liu, T. Qu, Y. Chen, H. Zhu, Y. Liu and G. Wu, Highly Dispersed Pd-CeO2 Nanoparticles Supported on N-Doped Core–Shell Structured Mesoporous Carbon for Methanol Oxidation in Alkaline Media, *ACS Catal.*, 2019, **9**, 6362-6371.
19. S. Lu, H. Li, J. Sun and Z. Zhuang, Promoting the methanol oxidation catalytic activity by introducing surface nickel on platinum nanoparticles, *Nano Res.*, 2018, **11**, 2058-2068.
20. Z. Zhang, Z. Luo, B. Chen, C. Wei, J. Zhao, J. Chen, X. Zhang, Z. Lai, Z. Fan, C. Tan, M. Zhao, Q. Lu, B. Li, Y. Zong, C. Yan, G. Wang, Z. J. Xu and H. Zhang, One-Pot Synthesis of Highly Anisotropic

Five-Fold-Twinned PtCu Nanoframes Used as a Bifunctional Electrocatalyst for Oxygen Reduction and Methanol Oxidation, *Adv. Mater.*, 2016, **28**, 8712-8717.

21. Y. Lou, C. Li, X. Gao, T. Bai, C. Chen, H. Huang, C. Liang, Z. Shi and S. Feng, Porous Pt Nanotubes with High Methanol Oxidation Electrocatalytic Activity Based on Original Bamboo-Shaped Te Nanotubes, *ACS Appl. Mater. Interfaces*, 2016, **8**, 16147-16153.
22. F. Ren, C. Wang, C. Zhai, F. Jiang, R. Yue, Y. Du, P. Yang and J. Xu, One-pot synthesis of a RGO-supported ultrafine ternary PtAuRu catalyst with high electrocatalytic activity towards methanol oxidation in alkaline medium, *J. Mater. Chem. A*, 2013, **1**, 7255-7261.